

# Neutron energy analysis by silicon prisms

J. Schulz<sup>1a</sup>, F. Ott<sup>b</sup>, Ch. Hülsen<sup>a</sup>, Th. Krist<sup>a</sup>

<sup>a</sup>*Helmholtz-Zentrum Berlin für Materialien und Energie, Hahn-Meitner-Platz 1, 14109  
Berlin, Germany*

<sup>b</sup>*Laboratoire Leon Brillouin, Bât 563 CEA Saclay, 91191 Gif sur Yvette Cedex, France*

---

## Abstract

Neutron energy analysing techniques allow to measure at different wavelengths at the same time thus avoiding losses due to monochromatization. We built and tested a refractive energy analysing device made from small prisms, where losses only occur due to the attenuation in the material.

We measured the refraction and the transmission of MgF<sub>2</sub> and Si prisms at the V14 reflectometer in Berlin at 4.9 Å to check their applicability. The experimentally determined linear attenuation coefficients are 0.055 cm<sup>-1</sup> for the MgF<sub>2</sub> and 0.03 cm<sup>-1</sup> for the Si prisms. An energy analyser consisting of silicon prism layers was measured at the EROS reflectometer at the LLB in a white neutron beam. The useful wavelength band was 2.4 to 7.6 Å. At 6.7 Å a wavelength resolution of 5% and a transmission of 53% were achieved. The surface roughness of the prisms could be determined to be (0.011 ± 0.006) deg.

*Keywords:* Neutron Optics, Energy analysis, Prisms

---

## 1. Introduction

2 Neutron reflectometry is an important technique to measure structure  
3 and composition close to the surface of a sample. There are principally two  
4 options to measure the ratio of the incoming and the reflected beam as a  
5 function of the wavevector transfer. In reflectometers working in time-of-  
6 flight mode a chopper is used to encode the neutron wavelengths in time and  
7 the incident angle of the neutron beam is fixed. The measurement of the

---

<sup>1</sup>Corresponding author. Tel.: +49 30 8062 43048.  
E-mail address: [jennifer.schulz@helmholtz-berlin.de](mailto:jennifer.schulz@helmholtz-berlin.de) (J. Schulz)

8 reflection is done for different wavelengths. In reflectometers working in the  
 9 monochromatic mode a crystal is used to select a fixed wavelength and the  
 10 measurement is performed at different angles.

11 Since the use of monochromators and choppers causes high losses in the  
 12 neutron flux, several optical elements had been investigated to substitute  
 13 these elements [1]. One option is to use a white beam and split the neutron  
 14 wavelengths in space. This can be accomplished by a magnetic field gradient  
 15 [2] or the refraction of the neutron beam in matter can be used [3][4], e.g.  
 16 the refraction by a row of prisms, as pioneered in the field of x-rays by W.  
 17 Jark [5].

## 18 2. Theory

19 Here we want to derive an expression for the wavelength resolution and  
 20 identify the effects contributing to the angular broadening of the neutron  
 21 beam.

22 For prism rows the refraction angle and thus the resolution increases with  
 23 the number of prisms. The angular dispersion of the system is the change  
 24 of the refracted angle according to the change in the index of refraction  $n$ ,  
 25 which is

$$n = 1 - \frac{\lambda^2}{2\pi} Nb, \quad (1)$$

26 where  $\lambda$  is the wavelength of the neutron and  $Nb$  the scattering length density  
 27 of the prism material. The refraction angle  $\varphi$  is given by Snells law

$$\varphi = \sin^{-1}(n \sin\alpha), \quad (2)$$

28 where  $\alpha$  is the incident angle. Since the angle increases in very good ap-  
 29 proximation linearly with the number of prism surfaces, the deflection of the  
 30 whole prism row is increased by a factor of 2 times the number of prisms  $i$ .  
 31 Thus the angular dispersion is

$$\frac{d\varphi_i}{d\lambda} \approx \frac{d(2i \sin^{-1}(n \sin(\alpha)))}{d\lambda} = 2i \frac{d\varphi_{i=1}}{d\lambda} \quad (3)$$

32 and the wavelength resolution of a prism system is given by

$$\frac{d\lambda}{\lambda} \approx \frac{d\varphi}{2i} \frac{(1 - n^2 (\sin\alpha)^2)^{1,5}}{(\sin\alpha)^3 n \frac{\lambda^2 Nb}{\pi}}. \quad (4)$$

33 The variable  $\varphi$  covers all effects that broaden the angular distribution of the  
 34 neutron beam. These effects are the incoming beam divergence  $\Theta_{Div}$  and the  
 35 scattering by surface roughness  $\Theta_{Rough}$ . Another effect is the total reflection  
 36  $\Theta_{Refl}$ , which occurs when the neutrons leave the prism layer they entered  
 37 and hit the flat back side of the next prism layer at an angle smaller than  
 38 the critical angle. If this angle is larger than the critical angle small angle  
 39 refraction occurs and broadens the beam by  $\Theta_{Refr}$ . At last the resolution of  
 40 the detector  $\Theta_{Det}$  also increases the effective broadening. Assuming Gaussian  
 41 distributions we get

$$d\varphi = \sqrt{\Theta_{Div}^2 + \Theta_{Det}^2 + \Theta_{Rough}^2 + \Theta_{Refl}^2 + \Theta_{Refr}^2}. \quad (5)$$

42 The transmitted intensity through the prisms is attenuated by absorption in  
 43 the material and scattering at the surfaces.  
 44 Following these considerations we designed an energy analyser made up of  
 45 prisms. For this purpose we used the Virtual Instrumentation Tool for the  
 46 European Spallation Source (VITESS) [8] for which a new module was writ-  
 47 ten. It simulates the refraction of neutrons by a given number of prisms and  
 48 takes into account all of the above mentioned effects except for the surface  
 49 scattering.

### 50 3. Choice of the material

51 We tested at the V14 neutron reflectometer at the HZB the applicability  
 52 of  $MgF_2$  and silicon as refraction materials, because they are available as  
 53 single crystals at reasonable prices and they show large ratios of refraction  
 54 to absorption of 5.25 for  $MgF_2$  and 0.86 for Si. Considering the scattering  
 55 on phonons [6] [7] these ratios decrease to 1.62 for  $MgF_2$  and 0.63 for silicon.  
 56 The  $MgF_2$  prism row consists of a  $50 \times 20 \times 2$  mm<sup>3</sup> single crystal block. The  
 57 upper 0.5 mm of the material are mechanically cut into the shape of 33 prisms,  
 58 each with an angle of 45 deg to the base of the prisms.

59 The silicon prism rows are produced by anisotropic etching. They consist  
 60 of 92 single prisms and cover an area of  $65 \times 50$  mm<sup>2</sup>. The height of each  
 61 prism is 0.5 mm. Since this is also the thickness of the raw material, there  
 62 is no unnecessary material in the beam path. We used (100) oriented silicon  
 63 wafers coated with silicon nitride. The prism structure was transferred by an  
 64 UV lithographic process to the silicon nitride layer. During the etch process  
 65 prisms with an angle of 54.7 deg to the basis were emerging.

66 We performed the measurements of refraction and transmission with a neu-  
67 tron beam of the wavelength 4.9 Å, a height of 0.3 mm and a divergence of  
68 0.006 deg. To detect the refracted beam a  $^3\text{He}$  detector with a slit of 0.2 mm  
69 at 2 m behind the prisms was moved across the beam. For the  $\text{MgF}_2$  prism  
70 row we found the maximum intensity of the refracted beam at 0.08 deg, see  
71 Fig.1, which corresponds to a refraction of 0.0024 deg per prism. This ex-  
72 perimental result is in good agreement with the theoretical calculation. The  
73 discrepancy of 8 % is due to mechanical imperfections of the prisms. The  
74 beam width increases while passing through the prisms by 0.015 deg com-  
75 pared to the FWHM of the direct beam.

76 For the  $^{92}\text{Si}$  prisms we found the maximum intensity at 0.058 deg (see Fig.  
77 2), which corresponds to a refraction of 0.0006 deg per prism. This result  
78 is as well in good agreement with the calculation. The discrepancy of 5 %  
79 is also caused by imperfections of the prisms. The beam width increases by  
80 0.005 deg compared to the FWHM of the direct beam.

81 To measure the transmission through the prism arrays the distance between  
82 sample and detector was reduced to 50 cm and the detector slit was removed.  
83 This increased the detector acceptance up to 2 deg which allows to cover the  
84 full refracted beam including the spread measured before. Through the 33  
85  $\text{MgF}_2$  prisms 86 % of all incoming neutrons were transmitted. This leads to  
86 an attenuation coefficient of  $\mu = 0.055 \text{ cm}^{-1}$ , which is about 83 % higher than  
87 the literature value including the phonon scattering [6]. The increase of the  
88 beam width and the high intensity losses indicate that the prisms surfaces  
89 are very rough and the neutrons are diffusely scattered.

90 The same measurement with  $^{92}\text{Si}$  prisms showed that 88 % of the neutrons  
91 are transmitted. The attenuation coefficient is  $\mu = 0.03 \text{ cm}^{-1}$ , which differs  
92 6 % from the literature value.

93 Since the widening of the refracted beam and its attenuation is much smaller  
94 for the Si than for the  $\text{MgF}_2$  prisms, we decided to build and test a prism  
95 energy analyser consisting of Si.

#### 96 4. Measurement of the refraction and resolution

97 We performed the measurement of the energy analyser at the time-of-  
98 flight reflectometer EROS at LLB. A stack of 4 Si prism rows, each with a  
99 height of 0.25 mm and made up from 191 single prisms, was put 2 m in front  
100 of a single  $^3\text{He}$  detector. The slit of the detector was set to 0.5 mm. The  
101 detector and the slit were moved in steps of 0.5 mm in the direction of the

102 refracted beam. The slit in front of the prisms was set to 0.3 mm height and  
103 the first slit 1800 mm upstream to 0.5 mm, so the beam divergence of the  
104 incoming beam was limited to 0.013 deg.

105 The measurement in the time-of-flight mode gives as a result the refracted  
106 intensity of the different wavelengths at certain detector positions. Putting  
107 the plots for all detector positions together, we get a two dimensional map,  
108 which shows the intensity distribution according to the detector positions  
109 and the neutron wavelengths, see Fig. 3. The coarse structure is an artifact  
110 due to the width of the slit and the step width of the detector. Below the  
111 main intensity of the refracted beam there is an area with low intensity, where  
112 neutrons are detected due to the total reflection and small angle refraction  
113 of the neutrons described above.

114 The measured wavelength distribution at each detector position has been  
115 fitted with an Gaussian function to extract the central wavelength and the  
116 FWHM. Fig. 4 shows the relation between wavelength and the detector angle.  
117 The data are in very good agreement with the data from a VITESS  
118 simulation.

119 Assuming Gaussian distributions the FWHM of the 1% wavelength res-  
120 olution of the chopper had been subtracted from the fitted FWHM of the  
121 measured wavelength distribution. Thus we determined the wavelength res-  
122 olution of the energy analyser to be 5% for 6.7 Å neutrons, see Fig. 5.

123 To quantify the effect of the diffuse scattering a fit with equation 4 and  $d\varphi$   
124 as the only free parameter was made, resulting in a value of 0.027 deg for  
125  $d\varphi$ .

126 By a VITESS simulation it was possible to give values for all terms in equa-  
127 tion 5. The value for  $\Theta_{Ref}$  is zero, because in the case of 191 prisms and  
128 for neutrons of wavelength smaller than 10 Å all refracted angles are smaller  
129 than the critical angle of Si, the effect of small angle refraction does not oc-  
130 cur.

131 Table 1 shows that the only cause of broadening which was not known or  
132 simulated, amounts to  $(0.011 \pm 0.006)$  deg. This part is caused by the scat-  
133 tering at the prisms surface and imperfections in the prisms structure. Its  
134 uncertainty is due to the uncertainty of the measured wavelength resolution.  
135 Fig. 6 shows that the experimental transmission of the neutrons varies be-  
136 tween 90% at 2.5 Å and 10% at 8 Å. A VITESS simulation shows that these  
137 losses of intensity are dominated by the total reflection of the neutrons at  
138 the back side of the prisms. With the prisms height of 0.25 mm all neutrons  
139 with wavelengths above 10 Å hit the back of the prisms in the layer above so

Term	Value [deg]
$\Theta_{Div}$	0.013
$\Theta_{Det}$	0.011
$\Theta_{Refr}$	0.000
$\Theta_{Refl}$	0.018

Table 1: Contribution of the different effects to the angular broadening of the beam.

140 the intensity of the beam transmitted within one prism layer reduces to zero,  
 141 since the totally reflected neutrons leave the prism rows at wrong angles.  
 142 This is a problem, because when a white beam is used only the projection  
 143 of the measured data (see Fig. 3) to the ordinate is available. To prevent to  
 144 detect neutrons at wrong angles it is possible to coat the prisms back side  
 145 with an absorbing layer. This does not reduce the intensity of the useful  
 146 neutrons and cleans up the signal in the detector.

147 With a bigger stack of prism rows it is possible to refract a larger white  
 148 beam without additional intensity losses due to the absorption in the mate-  
 149 rial. In comparison to the flat  $\text{MgF}_2$  prism presented by Cubitt [4] this is  
 150 an advantage but we would need 550 prisms at a wavelength of  $3.7 \text{ \AA}$  and  
 151 340 prisms at  $11 \text{ \AA}$  to achieve the same resolution. This increase of the to-  
 152 tal number of prisms would reduce the intensity of the useful beam to zero  
 153 due to the total reflection. A solution could be the bending of the prisms  
 154 optimized for the transmission of a selected wavelength band. This way the  
 155 distribution of the transmitted neutrons can be shifted to larger wavelengths  
 156 and its intensity increased.

## 157 5. Conclusion

158 It could be shown that due to the better surface quality of the prisms Si  
 159 is better suited as prism material than  $\text{MgF}_2$ .

160 The energy distribution of a neutron beam could be analyzed by a stack of  
 161 Si prism rows. We could achieve a resolution of better than 5 % for neutrons  
 162 with wavelengths longer than  $6.7 \text{ \AA}$ .

163 The transmission varies between 84 % for  $2.5 \text{ \AA}$  and 9 % for  $8 \text{ \AA}$ . These losses  
 164 are dominated by internal reflections of the neutrons, which additionally lead  
 165 to increased background. This problem can be overcome by coating the back  
 166 side of the prisms with an absorbing layer and by bending the prism rows.

167 The contribution of the surface roughness to the broadening of the angular

168 range could be determined to be  $(0.011 \pm 0.006)$  deg.

## 169 **Acknowledgements**

170 This research project has been supported by the European Commission  
171 under the 7th Framework Programme through "Research Infrastructures"  
172 action of the "Capacities" Programme, contract number CP-CSA-INFRA-  
173 2008-1.1.1. Number 226507-NMI3.

## 174 **References**

- 175 [1] F. Ott, A. Menelle, Eur. Phys. J. Special Topics 167, 93 (2009)
- 176 [2] F. Ott, A. de Vismes, Physica B 397, 153 (2007)
- 177 [3] R. Cubitt, et al., Nucl. Instrum. Meth. A 558, 547 (2006)
- 178 [4] R. Cubitt, et al., Eur. Phys. J. Plus 126, 111 (2011)
- 179 [5] W. Jark et al., J. Synchrotron Rad. 11, 248-253 (2010)
- 180 [6] J. G. Barker, et al., Journal of Applied Crystallography 41, 1003 (2008)
- 181 [7] A. W. Freund, Nucl. Instrum. Methods, 213, 495-501 (1983)
- 182 [8] VITeSS web site: [http://www.helmholtz-](http://www.helmholtz-berlin.de/forschung/grossgeraete/neutronenstreuung/projekte/vitess/index_de.html)  
183 [berlin.de/forschung/grossgeraete/neutronenstreuung/projekte/vitess/index\\_de.html](http://www.helmholtz-berlin.de/forschung/grossgeraete/neutronenstreuung/projekte/vitess/index_de.html)  
184 HZB (2012)

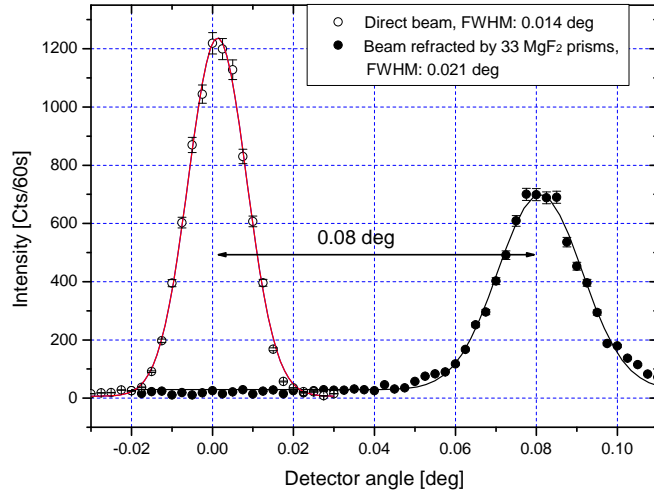


Figure 1: Refraction of a neutron beam with the wavelength  $4.9 \text{ \AA}$  by 33  $\text{MgF}_2$  prisms in comparison with the direct beam.

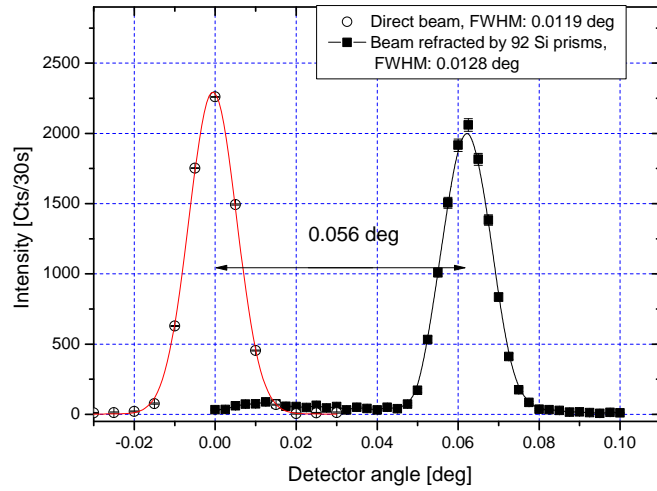


Figure 2: Refraction of a neutron beam with the wavelength  $4.9 \text{ \AA}$  by 92 Si prisms in comparison with the direct beam.



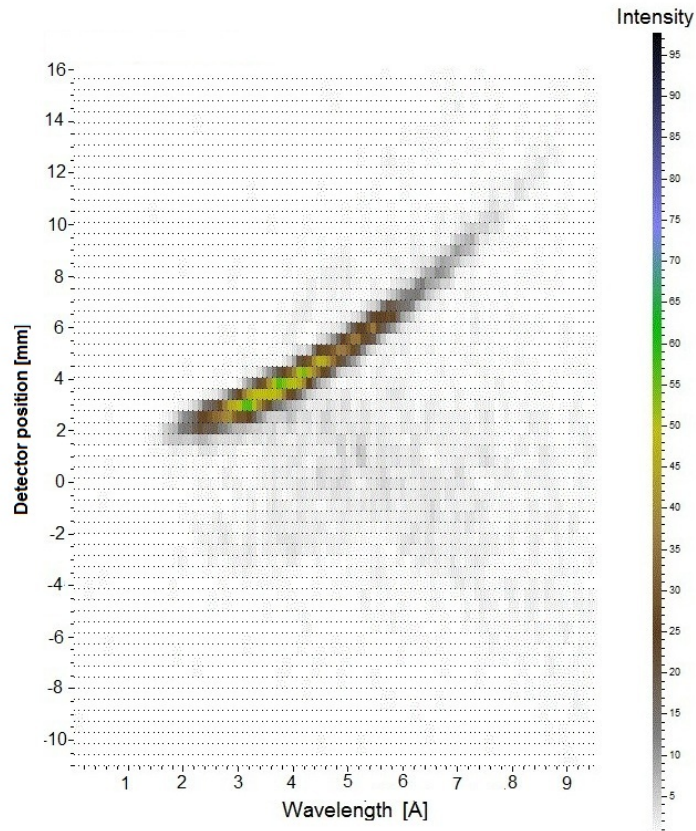


Figure 3: Measured intensity of the neutrons as a function of the neutron wavelength and the detector position after refraction by  $^{191}\text{Si}$  prisms. Due to the energy analyser each detector position encodes via the refracted angle the wavelength of the neutrons.

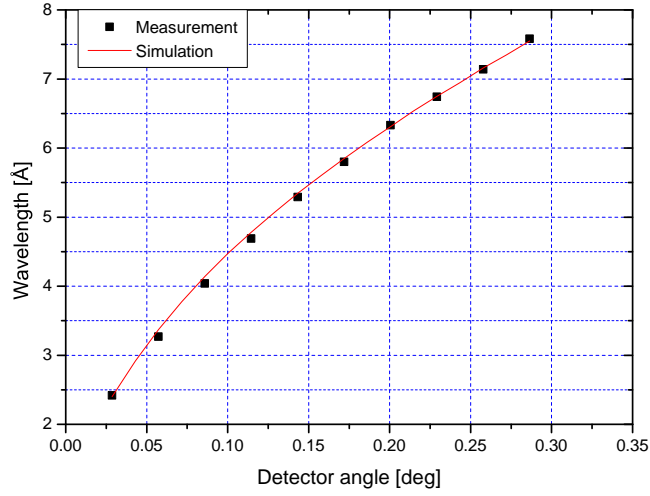


Figure 4: Measured main wavelength for each detector angle and the data from a VITESS simulation.

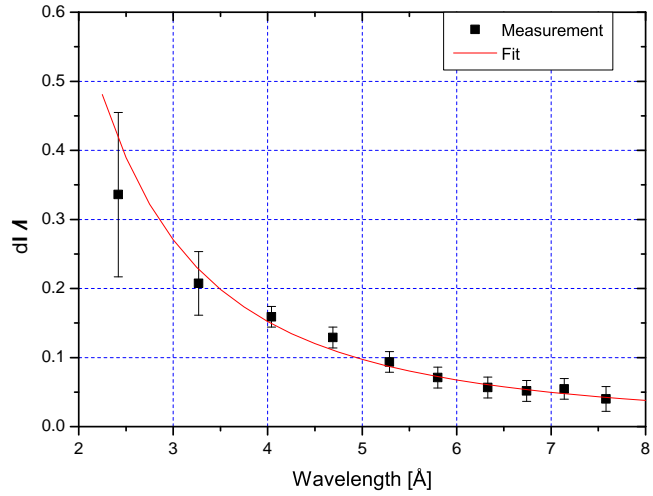


Figure 5: Experimental wavelength resolution of the energy analyser fitted with equation 4 and 5. The free parameter  $d\varphi$  was fitted to be 0.027 deg.

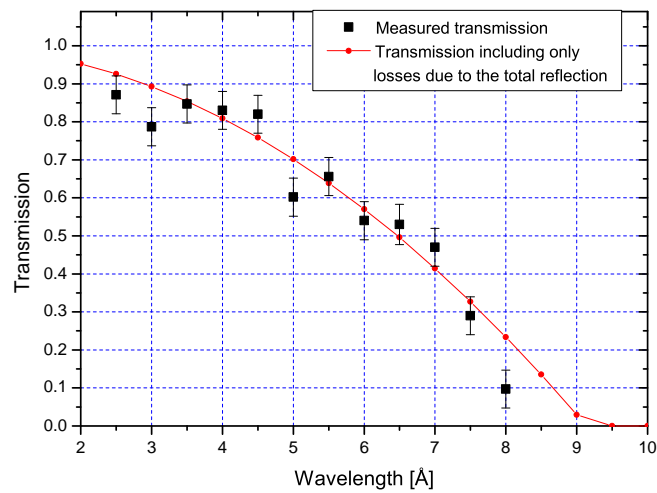


Figure 6: Measured transmission and calculated losses caused only by total reflection for 191 prisms.